FLIGHT TESTING AND ANALYSIS OF HELICOPTER GAS TURBINE ENGINE PERFORMANCE – A MULTIVARIABLE APPROACH

Ilan Arush, iarush@ntps.edu, National Test Pilot School (USA)
Marilena D. Pavel, m.d.pavel@TUdelft.nl, TU Delft (The Netherlands)

ABSTRACT

Helicopter performance flight-testing is an expensive activity that requires efficient testing techniques and appropriate data analysis for good performance prediction. Regarding the flight testing techniques used to evaluate the **available power** of a Turboshaft engine, current methodologies involve a simplistic single-variable polynomials analysis of the flight test data. This simplistic approach often results in unrealistic predictions. This paper proposes a novel method for analyzing flight-test data of a helicopter gas turbine engine. The so-called 'Multivariable Polynomial Optimization under Constraints' (MPOC) method is proven capable of providing an improved estimation of the engine maximum available power. The MPOC method relies on maximization of a multivariable polynomial subjected to both equalities and inequalities constraints. The Karush-Khun-Tucker (KKT) optimization technique is used with the engine operating limitations serving as inequalities constraints. The proposed MPOC method is implemented to a set of flight-test data of a Rolls Royce/Allison MTU250-C20 gas turbine, installed on a MBB BO-105M helicopter. It is shown that the MPOC method can realistically predict the engine output power under a wider range of atmospheric conditions and that the standard deviation of the output power estimation error is reduced from 13hp in the single-variable method to only 4.3hp using the MPOC method (over 300% improvement).

SYMBOLS AND ABBREVIATIONS

A = matrix containing numerical regressors
a_i, b_i, c_i = single variable polynomial coefficients
α_j^i = generic multivariable polynomial coefficient
$\vec{b}$ = vector to represent experimental CSHP
SHP = engine output power
$CSHP \triangleq SHP/\delta\sqrt{\theta}$ = corrected SHP (non-dimensional)
Ng = engine compressor speed.
$CNg \triangleq Ng/\sqrt{\theta}$ = corrected Ng (non-dimensional)
TGT = turbine gas temperature (engine temperature)
$CTGT \triangleq TGT/\theta$ = corrected TGT (non-dimensional)
W_f = engine fuel flow
$CW_f \triangleq W_f/\delta\sqrt{\theta}$ = corrected W_f (non-dimensional)
$\vec{E}_r$ = engine output power estimation error vector
$r_{x,y}$ = linear correlation between variables x,y
$VIF_{x,y} \triangleq \left(1 - r_{x,y}^2\right)^{-1}$ = variance inflation factor between x,y
δ = relative static ambient pressure
θ = relative static ambient temperature
f = generic multivariable function in x_i
g_j = inequalities constraints imposed on f
h_k = equalities constraints imposed on f
μ_j = Lagrange multipliers, inequalities constraints
λ_k = Lagrange multipliers, equalities constraints

1. INTRODUCTION

Flight test engineering is an interdisciplinary science with the objective of testing an aircraft or a system in its operational flight environment. For this, relying flight test data need to be gathered and reliable methods for data analysis need to be developed. There are many types of flight tests that can be performed, ex. performance assessment, structural integrity testing, handling qualities, flight envelope testing. This paper relates to performance flight testing, namely to the helicopter gas-turbine engine power testing methodology. Current methodology involves a simplistic single-variable polynomial analysis of the flight test data. This often results in unreliable estimation of the engine output power under a wider range of atmospheric conditions than those prevailed during the actual test (interpolation and extrapolation). A novel method is therefore proposed in the current paper involving a multivariable polynomial defined for the engine non dimensional parameters, i.e. Shaft Output Power, Compressor speed, Temperature and Fuel-Flow. The paper is structured as follows: after a short introduction, section II presents the current methodology for flight-test data analysis with respect to maximum available engine power. The current methodology is exemplified using flight test data of a BO-105M gas-turbine engine. In section III a novel methodology (referred to as the 'MPOC' method) is defined and demonstrated using the same flight test data of the BO-105M gas-turbine engine. Final

conclusions and recommendations complete the paper.

2. SINGLE VARIABLE ANALYSIS METHOD

2.1. Background

The useful performance of any helicopter depends on the amount by which the power available exceeds the power required [1]. The current method widely used for determining the maximum output power of an installed gas-turbine engine on a helicopter is based on recording stabilized engine(s) parameters (such as temperature, compressor speed, fuel-flow and shaft output power) accompanied by the atmospheric conditions prevailed during the test [2]. These flight-test data are gathered while flying the helicopter throughout its certified envelope and collecting engine parameters to their approved operating limitations. Once a substantial data base is gathered it can be analysed with the goal of deriving the maximum shaft output power the engine can deliver under various combinations of atmospheric conditions. One should keep in mind that the limiting factor for the maximum output power can change under different atmospheric conditions. For example, under hot day conditions the engine maximum output power could be limited by the engine temperature while under relatively cold day conditions the maximum engine compressor speed could limit the maximum power the engine can deliver. The data analysis methodology must provide both the maximum power and the associated limiting factor. Engine limiting factor can be either one of the following parameters: engine temperature, engine compressor speed, engine fuel-flow or the transmission torque. Dimensional analysis concepts are intensively used in performance flight-testing. Applying non-dimensional analysis tools reduces the number of dimensional parameters involved in the physical problem, and hence reduces substantially the number of flight-test sorties required, saving time and resources [3]. The first step in analyzing the engine data is related to correcting or non-dimensionalizing the raw flight-test data. There are mainly four engine parameters, i.e. shaft output power, compressor speed, temperature and fuel-flow which are corrected using the corresponding atmospheric conditions and are converted into CSHP, CNg, CTGT and CWf respectively. The mathematical procedure of non-dimensionalizing the gas turbine engine parameters is based on the Buckingham PI Theorem [4].

2.2. Single Variable Regression

Next phase is to apply common methods of linear regression in order to best fit three *separate single-*

variable polynomials as given by Eq. 1 to 3. These polynomials give the mathematical relation between the corrected engine power and each of the other corrected engine parameters. Common practice calls for these polynomials to be from the 3rd order so they can capture an inflection point representing an important physical characteristic of the engine. Each single-variable polynomial can be regarded as a 'finger-print' of the installed engine in the particular helicopter type and represents the dependency between the corrected output power and the single corrected engine parameter. As example throughout this paper consider the flight-test data gathered for a Rolls Royce/Allison MTU250-C20 gas turbine engine installed as the left engine on a MBB BO-105M helicopter. Applying Eq. 1 to 3 to this set of flight-test data and using least-squares technique results in Eq. 4 to 6. Figure 1 presents the three non-dimensional engine parameters plots for the example flight-test data.

(1) $$CSHP = f_1\left(CN_g\right) \approx b_0 + \sum_{i=1}^{3} b_i \left(CN_g\right)^i$$

(2) $$CSHP = f_2\left(CTGT\right) \approx a_0 + \sum_{i=1}^{3} a_i \left(CTGT\right)^i$$

(3) $$CSHP = f_3\left(CW_f\right) \approx c_0 + \sum_{i=1}^{3} c_i \left(CW_f\right)^i$$

(4) $$CSHP = f_1\left(CN_g\right) = -0.01\left(CN_g\right)^3 \\ +2.95\left(CN_g\right)^2 - 273.47\left(CN_g\right) + 8153.2$$

(5) $$CSHP = f_2\left(CTGT\right) = -3.3\times10^{-5}\left(CTGT\right)^3 \\ +0.07\left(CTGT\right)^2 - 43.87\left(CTGT\right) + 9256.7$$

(6) $$CSHP = f_3\left(CW_f\right) = -9.37\times10^{-6}\left(CW_f\right)^3 \\ +0.002\left(CW_f\right)^2 + 2.56\left(CW_f\right) - 234.3$$

2.3. The maximum available power

The final phase in this analysis is to evaluate the maximum available output power the engine is capable of delivering under a wide range of atmospheric conditions. For an atmospheric condition of choice, the engine output power is calculated separately in each path; the path of compressor speed limited engine by substituting the engine compressor speed limitation in Eq. 1, the path of temperature limited engine by substituting the engine maximum allowable temperature limitation in Eq. 2 and the path of fuel flow limited engine by substituting the engine fuel

flow limitation in Eq. 3. The three calculated values for the engine output power are then compared, first amongst themselves and then against the maximum transmission torque (transmission limitation). The maximum available power of the engine is assessed as the *minimum* out of all 4 paths described above [5].
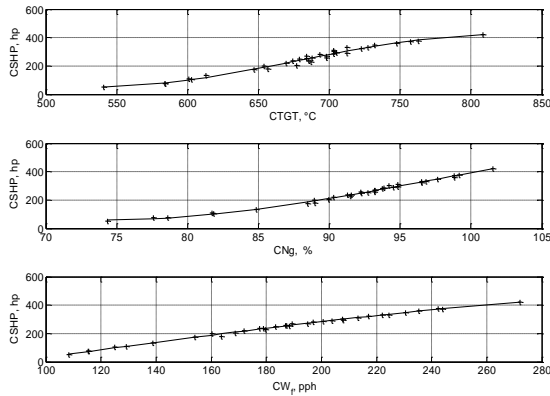

Figure 1. Non-Dimensional single-variable engine performance. Data represents 34 stabilized engine operation points during flight at various conditions.

The data presented in Fig. 2 were derived by following the described procedure with the example polynomials (Eq. 4, 5, 6). Figure 2 shows the analyzed data for up to 12,000 ft. of pressure-altitude and for five distinct day conditions; a standard day (ISA), 10°C and 20°C hotter than standard, 5°C and 10°C colder than standard day conditions. Figure 2 presents the *estimated* maximum continuous output power of the engine based on this set of flight test data. The continuous power rating of this type of engine was set at temperature of 738°C and compressor speed of 105%. For the fuel-flow a fictitious limitation (@ 450 pounds per hour) was used (since, for this specific engine and under atmospheric conditions used, this parameter of the engine is never a limiting factor). Another limitation mentioned above is the transmission limitation. This was at 344 hp for the continuous rating. It can be easily seen from Fig. 2 that for ISA, ISA-5 and ISA-10 day conditions the helicopter maximum power is transmission limited from sea level up to 790 ft., 2800 ft. and 3800 ft. of pressure altitude correspondingly. For higher pressure-altitudes the engine becomes temperature limited. As for a 10°C and 20°C hotter than standard day, analysis suggests the engine output power is temperature limited from sea level and above**.**
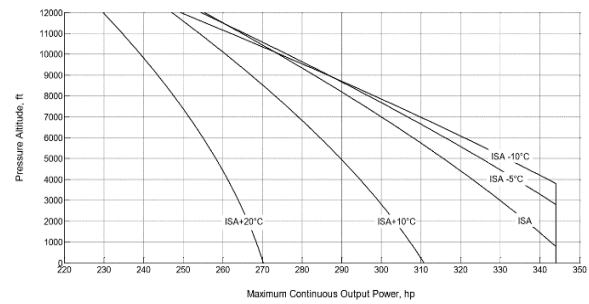

Figure 2. Estimated maximum continuous power of the example engine. Note the engine as installed in the helicopter is transmission limited for ISA, ISA-5 and ISA-10 conditions.

2.4.   Current method deficiency

The major flaw of this analysis method lies in the assumption of independency between the rules of operation in all three engine limiting factors. This drawback manifest itself by the unrealistic behavior of the three lines of ISA, ISA-5°C and ISA-10°C crossing each other above pressure-altitude of 8000 ft as seen in Fig. 2. It is physically impossible for a temperature limited engine to deliver more power whilst the ambient temperature is higher. The absolute errors between actual measured engine output power and the corresponding predicted values using the reduced polynomials (Eq. 4, 5, 6) are calculated using Eq. 7, 8 & 9 and presented in Fig. 3.
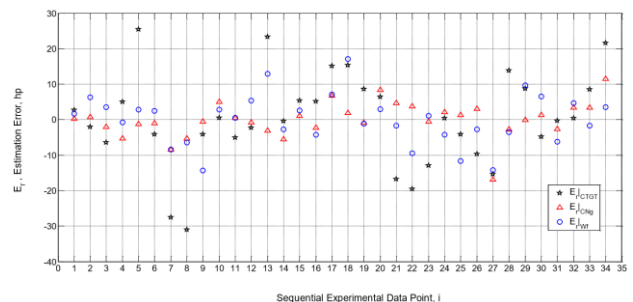

Figure 3. Engine output power estimation errors using single variable models. Note the relative large estimation errors of up to 30hp using the engine temperature variable.

These errors were found to be normally distributed about a *practically* zero mean. Figure 4 shows the errors standard deviation for each prediction path plotted against its relevant errors mean. This figure also includes a horizontal bar to represent the 95% confidence level interval range for the mean of the errors. One should realize that this bar shows where the mean of the prediction errors can be for a 95% confidence level. Looking at Fig. 4 one can see that the output power   based on engine

temperature (Eq. 4) yielded the worst performance; the relevant standard deviation of this error is 13hp and under 95% confidence level the mean of the estimation could be found anywhere along a range of ±4.6hp. A standard deviation of 13hp is considered a substantial error value for power predictions. Concluding, the current method used for determining the maximum output power of the helicopter gas-turbine engine can result in large errors and unrealistic predictions. Next section of the paper proposes a new method to improve gas-turbine flight-test data analysis.
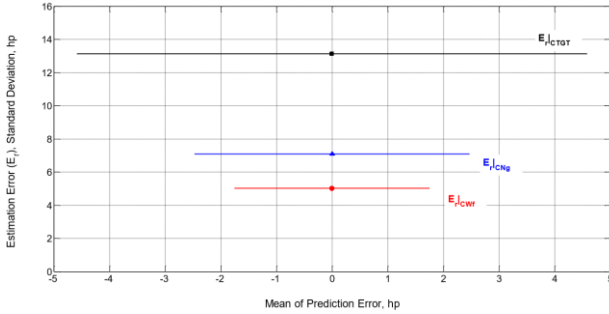

Figure 4. The mean and standard deviation of the single variable estimation errors. The engine temperature based estimation presented the worst performance with an error standard deviation of 13hp.

$$(7) \quad \vec{E}_r\Big|_{CNg} = \left\{ CSHP_i - f_1\left(CNg_i\right) \right\} \therefore i = 1,\dots 34$$

$$(8) \quad \vec{E}_r\Big|_{CTGT} = \left\{ CSHP_i - f_2\left(CTGT_i\right) \right\} \therefore i = 1,\dots 34$$

$$(9) \quad \vec{E}_r\Big|_{W_f} = \left\{ CSHP_i - f_3\left(W_{fi}\right) \right\} \therefore i = 1,\dots 34$$

3.   PROPOSED MULTIVARIABLE ANALYSIS METHOD

This section presents a novel analysis method referred to as 'Multivariable Polynomial Optimization under Constraints' (MPOC). This method requires no modification to the way engine performance flight-test sorties are carried out. First, a multivariable polynomial model to describe the engine output power is defined and evaluated for minimal multicollinearity. Once acquired a multivariable model to describe the engine output power based on the engine independent variables, the elegant method of *projection onto subspaces* is used to fit the model with experimental flight test data and to solve for the particular coefficients of the model. The maximum engine output power will be assessed as an optimization problem (maximization) under constraints. Since the case in hand has both equalities and inequalities constraints, the Karush-Khun-Tucker (KKT)

method which deals with both type of constraints will be implemented. The MPOC method presented in this chapter will be exemplified with the same flight-test data of the BO-105M left gas-turbine engine.

3.1. Search for a multivariable polynomial to describe the engine power

A *convenient* and *accurate* mathematical relationship needs to be found for representing the flight-test data. Polynomials serve a great role in flight-testing due to their simplicity and ease of manipulation. Different math model search algorithm are presented in the literature of specialty for optimizing regression models of experimental data obtained in aviation, see for example refs [6],[7],[8]. For the purpose of demonstrating the MPOC method, a simple 3rd order polynomial in all engine independent variables is suggested. The basic polynomial (Eq. 10) is augmented with only one predictor (f_1, f_2 or f_3) which involves a cross product between two independent engine parameters (Eq. 11). Using the example engine flight test data, the linear correlation (r) and the Variance Inflation Factor (VIF) between all three predictors are calculated (Eq. 12). The VIF between f_2 and f_3 was found to be 251, the VIF between f_1 and f_2 was 44 and the one between f_1 and f_3 was 36. For reasons of limiting the multicollinearity in the engine power model, f_1 was chosen to represent the other two cross product regressors (f_2 and f_3 - see Eq. 13).

$$
\begin{aligned}
CSHP_{M1} = {}& \alpha_1^1\left(CN_g\right)^3 + \alpha_2^1\left(CN_g\right)^2 + \alpha_3^1\left(CN_g\right) \\
(10) \quad & + \alpha_4^1\left(CTGT\right)^3 + \alpha_5^1\left(CTGT\right)^2 + \alpha_6^1\left(CTGT\right) \\
& + \alpha_7^1\left(CW_f\right)^3 + \alpha_8^1\left(CW_f\right)^2 + \alpha_9^1\left(CW_f\right) + \alpha_0^1
\end{aligned}
$$

$$
\begin{aligned}
(11) \quad & f_1 \triangleq \left(CN_g\right)\left(CTGT\right) \therefore f_2 \triangleq \left(CN_g\right)\left(CW_f\right) \\
& \therefore f_3 \triangleq \left(CTGT\right)\left(CW_f\right)
\end{aligned}
$$

$$
\begin{aligned}
(12) \quad & r_{x,y} \equiv \frac{\left(\dfrac{1}{n-1}\right) \cdot \sum\limits_{i=1}^{n}\left(xy\right) - n \cdot \bar{x} \cdot \bar{y}}{s_x \cdot s_y} \\
& \therefore VIF_{x,y} \equiv \frac{1}{1 - \left(r_{x,y}\right)^2}
\end{aligned}
$$

3.2. Fitting the candidate multivariable polynomial model with experimental data

This section presents the method used to fit the proposed multivariable model (Eq. 13) with the actual experimental flight-test data. The method

used is based on a linear Algebra concept known as *projection onto subspaces* [9]. The 34 flight-test data points of the exemplary gas-turbine engine are next substituted in Eq. 13. This produces a linear system of 34 equations with 11 unknowns (the coefficients α_n^2). This set of equations is compactly presented as Eq. 14. The matrix A is of the size of (34x11) and contains the numerical regressors as columns, α is a column vector (11x1) containing the unknown coefficients and b is a column vector (34x1) representing the measured experimental corrected output power of the engine (CSHP).

$$CSHP_{M2} = \alpha_1^2 \left(CN_g\right)^3 + \alpha_2^2 \left(CN_g\right)^2 + \alpha_3^2 \left(CN_g\right)$$

(13) $$+ \alpha_4^2 \left(CTGT\right)^3 + \alpha_5^2 \left(CTGT\right)^2 + \alpha_6^2 \left(CTGT\right) + \alpha_7^2 \left(CW_f\right)^3$$

$$+ \alpha_8^2 \left(CW_f\right)^2 + \alpha_9^2 \left(CW_f\right) + \alpha_{10}^2 \left(CN_g \cdot CTGT\right) + \alpha_0^2$$

(14) $$[A] \cdot \vec{\alpha} = \vec{b}$$

Substituting the regressors of the proposed candidate model into Eq. 14 results in Eq. 15

(15)

$$
\begin{bmatrix}
CNg_1^{\ 3} & CNg_1^{\ 2} & \cdot & \cdot & CNg_1 CTGT_1 & 1 \\
CNg_2^{\ 3} & CNg_2^{\ 2} & \cdot & \cdot & CNg_1 CTGT_1 & 1 \\
CNg_3^{\ 3} & CNg_3^{\ 2} & \cdot & \cdot & CNg_1 CTGT_1 & 1 \\
\cdot & \cdot & \cdot & \cdot & \cdot & \cdot \\
\cdot & \cdot & \cdot & \cdot & \cdot & \cdot \\
\cdot & \cdot & \cdot & \cdot & \cdot & \cdot \\
CNg_{33}^{\ 3} & CNg_{33}^{\ 2} & \cdot & \cdot & CNg_1 CTGT_1 & 1 \\
CNg_{34}^{\ 3} & CNg_{34}^{\ 2} & \cdot & \cdot & CNg_1 CTGT_1 & 1
\end{bmatrix}
\times
\begin{Bmatrix}
\alpha_1^2 \\ \alpha_2^2 \\ \alpha_3^2 \\ \alpha_4^2 \\ \alpha_5^2 \\ \alpha_6^2 \\ \alpha_7^2 \\ \alpha_8^2 \\ \alpha_9^2 \\ \alpha_{10}^2 \\ \alpha_0^2
\end{Bmatrix}
$$

$$
= \begin{Bmatrix}
CSHP_1 \\ CSHP_2 \\ CSHP_3 \\ \cdot \\ \cdot \\ \cdot \\ CSHP_{33} \\ CSHP_{34}
\end{Bmatrix}
$$

This system of equations is over-determined and does not have an exact solution. However, one can look for the 'closest' solution for this system, i.e. the 'best-fit' solution. This best-fit solution is denoted as $\{\hat{\alpha}\}$. The matrix constructed from $[\mathbf{A^T A}]^{-1}\mathbf{A^T}$ is the projection matrix which when multiplied by the vector b yields a solution in a subspace of A (Eq. 16). This solution serves as a best-fit or the closest solution one can determine. Following the above

described procedure one can solve for the 11 coefficients of Eq. 15 using Eq. 17.

(16) $$\{\hat{\alpha}\} = \left[A^T A\right]^{-1} A^T \cdot \vec{b}$$

(17) $$\{\alpha_i^1\} = \left[A^T A\right]^{-1} A^T \cdot \{CSHP\}$$

For completeness of this procedure presentation, the particular solution obtained using all 34 test data points of the BO-105 example engine is given by Eq. 18.

(18) $$\{\alpha_i^2\} \triangleq \begin{Bmatrix} \alpha_1^2 \\ \alpha_2^2 \\ \alpha_3^2 \\ \alpha_4^2 \\ \alpha_5^2 \\ \alpha_6^2 \\ \alpha_7^2 \\ \alpha_8^2 \\ \alpha_9^2 \\ \alpha_{10}^2 \\ \alpha_0^2 \end{Bmatrix} = \begin{Bmatrix} -0.0165 \\ 3.837 \\ -380.69 \\ 3.36\times10^{-5} \\ -0.075 \\ 41.809 \\ -8.35\times10^{-5} \\ 0.043 \\ -5.577 \\ 0.1486 \\ 2242.4 \end{Bmatrix}$$

3.3. Statistical validity of the proposed candidate multivariable polynomial model

Consider the prediction errors of the proposed engine power model per an experimental data point as presented in Fig. 5 and calculated according to Eq. 19. For comparison, Fig. 5 also includes partial data obtained from single variable analysis method. Looking at Fig. 5 one can perceive that the proposed model (Eq. 13, 18) performs much better in predicting the engine output power as compared to the single variable polynomial based on the corrected engine temperature (CTGT). Prediction errors of the proposed multivariable model were found to be approximately normally distributed about a *practically* zero mean (the precise mean was 3.9×10^{-10} hp). This normality of the prediction errors can be demonstrated by the roughly straight line of the normal Quantile-Quantile plot (Q-Q plot) presented as Fig. 6.

(19) $$\vec{E}_r\Big|_{M2} = \{CSHP_i - (CSHP_{M2})_i\} \therefore i = 1,2,3,\dots,34$$

(20) $$t_{M2} = \frac{\overline{\left(\vec{E}_r\big|_{M2}\right)}}{s/\sqrt{n}}$$

The P-value analysis: The concept behind the P-*value* is thoroughly discussed in literature [10]. In a nutshell, it is based on stating an hypothesis (the *Null Hypothesis*, H_0) that is then supported or rejected based on statistical analysis of the experimental data. For the engine analysis, H_0 is set to claim that the proposed multivariable model produces an array of estimation errors with a zero *mean*. The P-value returned represents the *smallest* significant level that leads to falsely rejecting the Null Hypothesis while it is valid (type I error). This is the reason for low P-values to cast doubt on the validity of the null hypothesis and leads to the acceptance of the alternative hypothesis. The prediction errors of the proposed multivariable model presented in Fig. 5 can be replaced with a single value to encapsulate the entire performance of the model. This value is the test-statistic and is calculated using the mean of prediction errors divided by the estimated population standard deviation (Eq. 20).
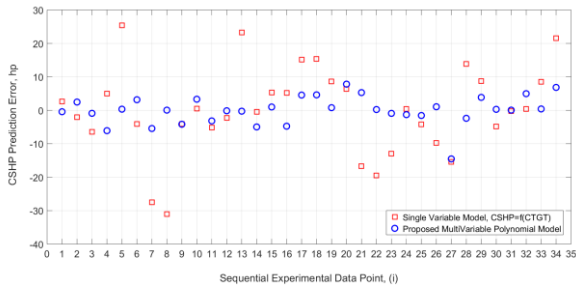

Figure 5. *Estimation errors comparison between the proposed multivariable engine power model and the single variable model based on the engine temperature.*

One should realize that low test-statistic values return large P-values and vice versa. The test-statistic of the proposed model (Eq. 13,18) was calculated to be an extremely low value of 1.5×10^{-11} which returned a calculated P-value of 1. The practical conclusion of this analysis is that it can be stated, with a confidence level of above 99%, that the multivariable polynomial model proposed (Eq. 13,18) predicts the BO-105M engine
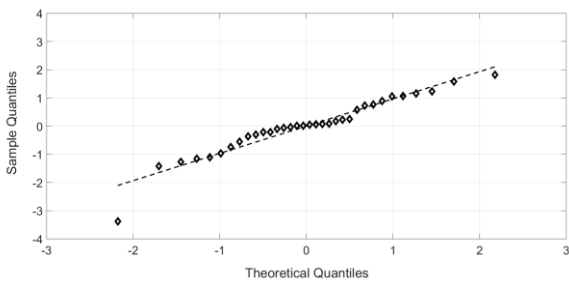

Figure 6. *Normal Quantile-Quantile (Q-Q) plot for the prediction errors of the proposed multivariable engine model.*

power with normally distributed prediction errors about a zero mean (the *Null Hypothesis,* H_0).

3.4. Estimation of the maximum output power using the MPOC analysis approach

Once acquiring a multivariable polynomial to describe the change in corrected engine output power based on other engine corrected parameters (compressor speed, temperature and fuel-flow), Eq. 13, 18 for the specific flight test data presented in this paper, one can predict the maximum available output power of the engine under various atmospheric conditions. The engine output power is limited by reaching one (or more) of its independent parameters. Finding the maximum output power is equivalent with finding an extremum point (maximum output power) under constraints (the engine independent parameters: compressor speed, temperature or fuel-flow). Finding an extremum point of a multivariable function under constraints is of a different nature from the case of a single variable function. The most popular approach for the multivariable case is using Lagrange multipliers but this approach applies only to equalities constraints only whereas the problem we have in hand involves both equalities and inequalities constraints. One possible approach for optimization under both equalities and inequalities constraints is the KKT (Karush-Kuhn-Tucker) method [11]. Eq. 21 presents the Lagrange equations required for satisfying extremum points of a multivariable function $f(x_i)$ subjected to 'm' number of inequalities constraints, $g(x_i)$ and 'l' number of equalities constraints, $h(x_i)$. μ_j represent the Lagrange multipliers associated with the *inequalities* constraints and λ_k represent the Lagrange multipliers associated with the *equalities* constraints.

(21)
$$\frac{\partial f}{\partial x_i} + \sum_{j=1}^{m}\left(\mu_j \frac{\partial g_j}{\partial x_i}\right) + \sum_{k=1}^{l}\left(\lambda_k \frac{\partial h_k}{\partial x_i}\right) = 0 \therefore i = 1,2,3,...,n$$
$$x = \left[x_1, x_2,...,x_n\right]$$
$$g_j(x) \le 0 \therefore \left(j = 1,2,...,m\right)$$
$$h_k(x) = 0 \therefore \left(k = 1,2,...,l\right)$$

The function to be maximized is the proposed model (Eq. 13, 18) subjected to several constraints. The system of equations (Eq. 21) can be solved when at least two *equality* constraints are provided. Those are fulfilled with the engine internal rule of operation, as explained hereinafter. Applying similar statistical tools as described in section 3.3, a best fit surface is calculated constituting the engine multivariable *internal rule of operation*. This surface which describes the relationship of the corrected engine temperature with both corrected

compressor speed and corrected fuel-flow, is complemented by the experimental data points and is presented in Fig. 7. Looking at Fig. 7 one can see that the surface plotted covers a much larger range than it should (it is extrapolated) and this is done only for visualization. Based on the surface in Fig. 7 two constraints are selected:

1) The first one is denoted as h_1 and is represented in its implicit form as Eq. 22 relating the corrected engine temperature to the corrected compressor speed.

2) The second is denoted as h_2 and represents the relationship between the corrected compressor speed and the corrected fuel-flow (Eq. 23).

Note that both h_1 and h_2 constraints are projections of the multivariable rule of operation onto two planes; the CTGT-CNg plane and the CNg-CW$_f$ plane respectively.
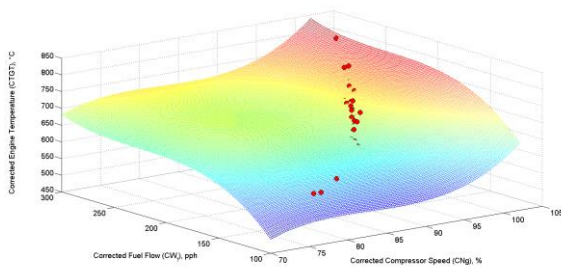

Figure 7. *The engine multivariable internal rule of operation. The relationship between the corrected engine temperature and the corrected values of the engine compressor speed and fuel flow. The circles presented are the experimental data points, which some are obscured by the best fit surface.*

(22) $h_1 : CTGT - a_1 (CNg)^3 - a_2 (CNg)^2 - a_3 (CNg) - a_4 = 0$

$$\therefore \begin{pmatrix} a_1 \\ a_2 \\ a_3 \\ a_4 \end{pmatrix} = \begin{pmatrix} 0.0117 \\ -2.9739 \\ 258.49 \\ -7050 \end{pmatrix}$$

(23) $h_2 : CNg - b_1 (CWf)^3 - b_2 (CWf)^2 - b_3 (CWf) - b_4 = 0$

$$\therefore \begin{pmatrix} b_1 \\ b_2 \\ b_3 \\ b_4 \end{pmatrix} = \begin{pmatrix} 6.492 \times 10^{-6} \\ -0.00433 \\ 1.0621 \\ 2.9888 \end{pmatrix}$$

The *inequalities* constraints for the engine

maximum output power are simply the operational limitations imposed on the engine. For the example BO-105 engine these are the continuous rating of the engine and are represented as Eq. 24, 25 and 26.

(24) $g_1 : CNg - \dfrac{105}{\sqrt{\theta}} \leq 0$

(25) $g_2 : CTGT - \dfrac{738}{\theta} \leq 0$

(26) $g_3 : CW_f - \dfrac{450}{\delta\sqrt{\theta}} \leq 0$

The partial differential equations (Eq. 21) and the KKT conditions (Eq. 24 to 26) for a *maximization* problem result in Eq. 27, 28 and 29.

(27) $\dfrac{\partial(CSHP_{M2})}{\partial(CNg)} - \mu_1 + \lambda_1 \dfrac{\partial(h_1)}{\partial(CNg)} + \lambda_2 = 0$

(28) $\dfrac{\partial(CSHP_{M2})}{\partial(CTGT)} - \mu_2 + \lambda_1 = 0$

(29) $\dfrac{\partial(CSHP_{M2})}{\partial(CW_f)} - \mu_3 + \lambda_2 \dfrac{\partial(h_2)}{\partial(CWf)} = 0$

Equations 27, 28 and 29 can be rearranged as Eq. 30.

(30)
$$\begin{pmatrix} \dfrac{\partial(CSHP_{M2})}{\partial(CNg)} \\[2ex] \dfrac{\partial(CSHP_{M2})}{\partial(CTGT)} \\[2ex] \dfrac{\partial(CSHP_{M2})}{\partial(CW_f)} \end{pmatrix} = \begin{pmatrix} 1 & 0 & 0 & -\dfrac{\partial(h_1)}{\partial(CNg)} & -1 \\[1ex] 0 & 1 & 0 & -1 & 0 \\[1ex] 0 & 0 & 1 & 0 & -\dfrac{\partial(h_2)}{\partial(CW_f)} \end{pmatrix} \cdot \begin{pmatrix} \mu_1 \\ \mu_2 \\ \mu_3 \\ \lambda_1 \\ \lambda_2 \end{pmatrix}$$

The set of partial differential equations (Eq. 30) describe conditions for candidate engine corrected parameters representing maximization of the engine output power. This set does not have a unique solution but a solution with 2 degrees of freedom for the three different cases it represents (5 unknowns with only 3 equations). The first case (Case I) is when the compressor speed is at its maximum value, i.e., the engine output power is limited by the compressor speed. The second case (Case II) is when the output power is limited by the engine temperature and the third case (Case III) is a fuel-flow limited engine. Separating Eq. 30 into the three individual cases and applying the KKT conditions on the Lagrange multipliers associated with the inequalities constraints (μ_1, μ_2, μ_3)

eliminates the two degrees of freedom and makes each one of these cases to have a unique solution.

3.4.1. Case I – Compressor speed limited engine

Applying the KKT conditions for Case I imposes the following conditions on the Lagrange multipliers associated with the inequalities constraints (Eq. 31).

(31) $\{\mu_1 > 0, \mu_2 = 0, \mu_3 = 0\}$

Combining Eq. 31 and Eq. 30 results in the system of equations (Eq. 32), i.e.

$$
\begin{pmatrix} \dfrac{\partial(CSHP_{M2})}{\partial(CNg)} \\ \dfrac{\partial(CSHP_{M2})}{\partial(CTGT)} \\ \dfrac{\partial(CSHP_{M2})}{\partial(CWf)} \end{pmatrix} = \begin{pmatrix} 1 & -\dfrac{\partial(h_1)}{\partial(CNg)} & -1 \\ 0 & -1 & 0 \\ 0 & 0 & -\dfrac{\partial(h_2)}{\partial(CWf)} \end{pmatrix} \cdot \begin{pmatrix} \mu_1 \\ \lambda_1 \\ \lambda_2 \end{pmatrix}
$$

(32)
$$
\therefore \begin{cases} \mu_1 > 0 \\ CNg = \dfrac{105}{\sqrt{\theta}} \\ CTGT < \dfrac{738}{\theta} \\ CWf < \dfrac{450}{\delta\sqrt{\theta}} \end{cases}
$$

3.4.2. Case II – Temperature limited engine

Applying the KKT conditions for Case II imposes the following conditions on the Lagrange multipliers associated with the inequalities constraints (Eq. 33).

(33) $\{\mu_1 = 0, \mu_2 > 0, \mu_3 = 0\}$

Substituting Eq. 33 into Eq. 30 results in equations (Eq. 34), i.e.

$$
\begin{pmatrix} \dfrac{\partial(CSHP_{M2})}{\partial(CNg)} \\ \dfrac{\partial(CSHP_{M2})}{\partial(CTGT)} \\ \dfrac{\partial(CSHP_{M2})}{\partial(CWf)} \end{pmatrix} = \begin{pmatrix} 0 & -\dfrac{\partial(h_1)}{\partial(CNg)} & -1 \\ 1 & -1 & 0 \\ 0 & 0 & -\dfrac{\partial(h_2)}{\partial(CWf)} \end{pmatrix} \cdot \begin{pmatrix} \mu_2 \\ \lambda_1 \\ \lambda_2 \end{pmatrix}
$$

(34)
$$
\therefore \begin{cases} \mu_2 > 0 \\ CNg < \dfrac{105}{\sqrt{\theta}} \\ CTGT = \dfrac{738}{\theta} \\ CWf < \dfrac{450}{\delta\sqrt{\theta}} \end{cases}
$$

3.4.3. Case III – Fuel flow limited engine

Case III is when the maximum output power of the engine is bounded by reaching the maximum fuel-flow the pump is capable of delivering to the engine. Applying the KKT conditions for this case imposes the following conditions on the Lagrange multipliers associated with the inequalities constraints (Eq. 35).

(35) $\{\mu_1 = 0, \mu_2 = 0, \mu_3 > 0\}$

Combining Eq. 35 with Eq. 30 results in the set of equations (Eq. 36), i.e.

$$
\begin{pmatrix} \dfrac{\partial(CSHP_{M2})}{\partial(CNg)} \\ \dfrac{\partial(CSHP_{M2})}{\partial(CTGT)} \\ \dfrac{\partial(CSHP_{M2})}{\partial(CWf)} \end{pmatrix} = \begin{pmatrix} 0 & -\dfrac{\partial(h_1)}{\partial(CNg)} & -1 \\ 0 & -1 & 0 \\ 1 & 0 & -\dfrac{\partial(h_2)}{\partial(CWf)} \end{pmatrix} \cdot \begin{pmatrix} \mu_3 \\ \lambda_1 \\ \lambda_2 \end{pmatrix}
$$

(36)
$$
\therefore \begin{cases} \mu_3 > 0 \\ CNg < \dfrac{105}{\sqrt{\theta}} \\ CTGT < \dfrac{738}{\theta} \\ CWf = \dfrac{450}{\delta\sqrt{\theta}} \end{cases}
$$

3.4.4. Demonstration of Case II – Temperature limited engine

The next section demonstrates the specifics of Case II using the example BO-105 flight-test data.

Similar methodology can be applied to find the maximum output power for the other two cases. The set of equations specified in Eq. 34 has a solution if and only if the rank of the system matrix equals the rank of the auxiliary matrix. This solution is also unique if both ranks equal three (i.e., the three Lagrange multipliers). This requirement for a unique solution can be stated mathematically as Eq. 37.

$$rank \begin{pmatrix} 0 & -\dfrac{\partial(h_1)}{\partial(CNg)} & -1 \\ 1 & -1 & 0 \\ 0 & 0 & -\dfrac{\partial(h_2)}{\partial(CWf)} \end{pmatrix} =$$

(37)

$$= rank \begin{pmatrix} 0 & -\dfrac{\partial(h_1)}{\partial(CNg)} & -1 & \dfrac{\partial(CSHP_{M2})}{\partial(CNg)} \\ 1 & -1 & 0 & \dfrac{\partial(CSHP_{M2})}{\partial(CTGT)} \\ 0 & 0 & -\dfrac{\partial(h_2)}{\partial(CWf)} & \dfrac{\partial(CSHP_{M2})}{\partial(CWf)} \end{pmatrix} = 3$$

Instead of searching for a pair of corrected compressor speed and corrected fuel-flow under a limited corrected temperature ($CTGT_{limit}$) to satisfy Eq. 34, one can simplify the process by using an engineering approach: for each and every combination of atmospheric conditions a pair of candidate corrected compressor speed and corrected fuel-flow are suggested via the engine internal rule of operation (Eq. 22 and 23). These candidate pairs complemented by the engine temperature limit will then be evaluated for realisation of the KKT conditions required for maximization of the engine output power. Since the equations specified in Eq. 34 have a unique solution, they can be rearranged as in Eq. 38. The three engine parameters (candidates for maximum output power) can be used in Eq. 38 to solve for the Lagrange multipliers. The three candidate simultaneous engine independent parameters will be valid for defining a maximum output power of a temperature limited engine if and only if the solution of Eq. 38 is achieved while coinciding with the KKT conditions required for the case. This procedure was carried out using the engine internal rules of operation (Eq. 22 and 23) for different day conditions (ISA, ISA+10°C, ISA+20°C, ISA-5°C & ISA-10°C). Figure 8 presents the maximum output power of the example engine along with all the KKT requirements as a function of pressure altitude for an ISA day conditions. It can be seen that all the KKT requirements are met. Figure 9 presents the

maximum continuous output power of the engine as a function of pressure-altitude for different day conditions. The maximum continuous output power of the engine is temperature limited under all atmospheric conditions, see Fig. 9. Note the KKT requirements were omitted from Fig. 9 although they were all met.
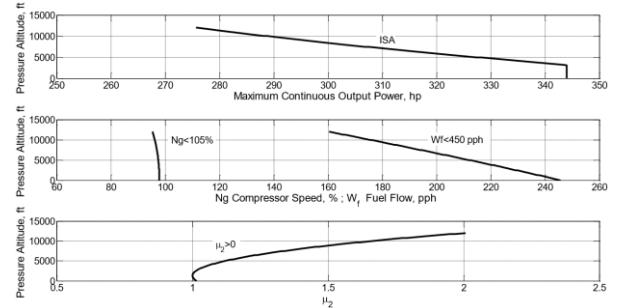

Figure 8. A simultaneously presentation of all engine parameters for pressure-altitude between sea level and 12,000 ft. under standard day conditions (ISA). The engine is temperature limited at 738°C. Note the fulfillment of all KKT conditions for output power maximization of the temperature-limited engine..

$$\begin{pmatrix} \mu_2 \\ \lambda_1 \\ \lambda_2 \end{pmatrix} = \begin{pmatrix} \dfrac{-1}{(\partial h_1/\partial CNg)} & 1 & \dfrac{1}{(\partial h_1/\partial CNg)(\partial h_2/\partial CW_f)} \\ \dfrac{-1}{(\partial h_1/\partial CNg)} & 0 & \dfrac{1}{(\partial h_1/\partial CNg)(\partial h_2/\partial CW_f)} \\ 0 & 0 & \dfrac{-1}{(\partial h_2/\partial CW_f)} \end{pmatrix} \cdot \begin{pmatrix} \dfrac{\partial(CSHP_{M2})}{\partial(CNg)} \\ \dfrac{\partial(CSHP_{M2})}{\partial(CTGT)} \\ \dfrac{\partial(CSHP_{M2})}{\partial(CWf)} \end{pmatrix}$$

(38)

$$\therefore KKT : \begin{cases} \mu_2 > 0 \\ CNg < \dfrac{105}{\sqrt{\theta}} \\ CTGT = \dfrac{738}{\theta} \\ CWf < \dfrac{450}{\delta\sqrt{\theta}} \end{cases}$$

4. COMPARISON OF MAXIMUM OUTPUT POWER FOR THE CURRENT AND THE MPOC METHODS

The estimated maximum engine output power is compared using both the current and the proposed MPOC methods as seen in Fig. 10. Looking at this figure it follows that both methods demonstrate similar results for atmospheric conditions close to those prevailed during the actual flight-tests (ISA+21°C); however, while the current single-variable method completely collapsed under ISA and colder day conditions, the MPOC method

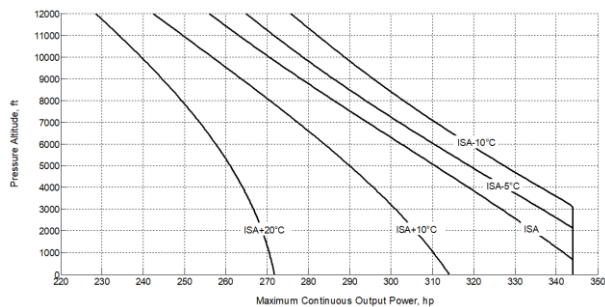predicted reasonable and logical estimations for ISA and colder day conditions.

Figure 9. *Estimation of the engine maximum continuous output power between sea level to 12,000 ft. under different day conditions. The maximum continuous power of the engine was estimated to be temperature limited. Note the engine maximum continuous power for ambient temperatures of a standard day profile (ISA) and below is bounded by the helicopter transmission rating.*
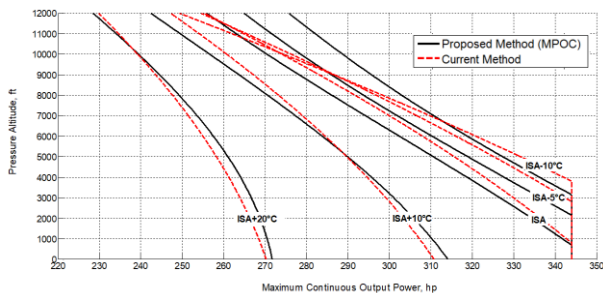

Figure 10. *Comparison between the proposed and the current methods. It can clearly be seen that while the current single variable method collapses under the estimation for maximum continuous output power for standard day conditions and colder, the proposed multivariable method still provides a logical estimation.*

5. CONCLUSIONS

The output power of a helicopter gas turbine engine is a multivariable problem that can be non-dimensionalized. Oversimplification of the problem as linear combination of single-variable models does *not* provide sufficient accuracy and frequently provides unrealistic estimations for the maximum output power under atmospheric conditions different than those prevailed during flight testing. The method presented in this paper (Multivariable Polynomial Optimization under Constraints, MPOC) is based on *multivariable* polynomials. This method proves substantial better performance in estimating the output power of a BO105 helicopter used as example in this paper (over 300% of improvement).For MPOC method practical application, the paper proposes a multivariable

polynomial of the third order. Selection of a particular model of this multivariable polynomial is based on minimization of collinearity between the variables and sufficient P-values returned. This specific model is probably not deemed as the best possible for the relevant task but it is a first possible solution. Predicting the maximum output power of a gas turbine engine can be regarded, mathematically, as an optimization problem of a multivariable function subjected to both equalities and inequalities constraints. The equalities constraints should be based on the flight test data and the inequalities are provided by the engine operating limitations. Although the current single-variable method used for assessing helicopter gas-turbine power available is simple, one should utilize it only as a first estimation and not as an accurate flight testing analysis tool in the process of estimating the maximum output power of a gas-turbine engine. The approach presented in this paper will be expanded in the future to include flight test data from other types of helicopters and engines. Future research can also include a comparative analysis between a broader base of candidate multivariable engine models in order to better understand which type of regressors are a better choice for the task of modelling the output power of helicopter gas turbine engines.

REFERENCES

[1] Advisory Group for Aerospace Research & Development (AGARD), *Flight Test Techniques Series.* AGARD-AG-300, 1995.

[2] Cooke, A.K. and Fitzpatrick EWH, *Helicopter Test and Evaluation*, 1st ed., AIAA Education Series, 2002.

[3] Knowles, P. *The Application of Non-dimensional Methods to the Planning of Helicopter Performane Flight Trials and Analysis Results,* Aeronautical Research Council ARC CP 927, 1967.

[4] Buckingham, E., "On Physically Similar Systems; Illustrations of the Use of Dimensional Equations," *Physical Review*, Vol. IV, No. 4, 1914,

pp. 345, 376, doi: 10.1103/PhysRev.4.345.

[5] National Test Pilot School, *Professional Course Textbook Series, Vol. VII, Rotary Wing Performance Flight Testing,* Mojave, 2017, Chap. 5.

[6] Ulbrich, N., Regression Model Optimization for the Analysis of Experimental Data, AIAA 2009–1344, paper presented at the 47th AIAA Aerospace Sciences Meeting and Exhibit, Orlando, Florida, January 2009.

[7] Ulbrich, N., Optimization of Regression Models of Experimental Data using Confirmation Points, AIAA 2010–930, paper presented at the 48th AIAA Aerospace Sciences Meeting and Exhibit, Orlando, Florida, January 2010.

[8] Zhao, D. and Xue, D., A multi-surrogate approximation method for metamodeling, *Engineering with Computers,* Vol. 27, No. 2, pp. 139-153, 2011.

[9] Strang, G., *Introduction to Linear Algebra*, 5th ed., Wellesley-Cambridge Press, Wellesley MA, 2016, Chap. 4.

[10] Guttman, I., Wilks, S., and Hunter, J., *Introductory Engineering Statistics*, 2nd ed., John Wiley & Sons, Inc., New York, 1971, Chap. 10.

[11] Singiresu, R., *Engineering Optimization Theory and Practice*, 4th ed., John Wiley & Sons, Inc., New Jersey, 2009, Chap. 2.